AQUA
Water Infrastructure, Ecosystems and Society

 AQUA — Water Infrastructure, Ecosystems and Society Vol 72 No 8, 1629 doi: 10.2166/aqua.2023.316

Recent advancement in $NiFe_2O_4$-based nanocomposites for the photocatalytic degradation of pollutants in aqueous solutions: a comprehensive systematic review

Elham Derakhshani[a] and Ali Naghizadeh[b,]*

[a] PhD Candidate of Environmental Health Engineering, Student Research Committee, Medical Toxicology and Drug Abuse Research Center (MTDRC), Birjand University of Medical Sciences (BUMS), Birjand, Iran
[b] Medical Toxicology and Drug Abuse Research Center (MTDRC), Birjand University of Medical Sciences (BUMS), Birjand, Iran
*Corresponding author. E-mail: al.naghizadeh@yahoo.com

ABSTRACT

Nanocomposites with diameters of 1 to 100 nm have modified properties such as uniform size distribution, small size, high surface-to-volume ratio, high absorbability, porosity, and various potential roles, including in catalytic and biological activities. The purpose of this research study was to systematically review all research studies on the photocatalytic decomposition of pollutants by $NiFe_2O_4$-based nanocomposites and evaluate the optimal laboratory conditions and the results of these studies. The present systematic review was conducted by searching Scopus, PubMed and Web of Science databases until March 2022. The parameters of nano catalyst type and size, synthesis methods, pollutant type, optimal pH, optimal initial pollutant concentration, optimal catalyst concentration, optimal time, radiation and removal efficiency were investigated. 454 studies were screened and using the inclusion and exclusion criteria, in total, 31 studies met our inclusion criteria and provided the information necessary to photocatalytic degradation of pollutants by $NiFe_2O_4$-based nanocomposites. In the investigated studies, the percentage of photocatalytic degradation of pollutants by $NiFe_2O_4$-based nanocomposites was reported to be above 70%, and in some studies, the removal efficiency had reached 100%. From the results of this systematic review, it was concluded that the photocatalytic process using $NiFe_2O_4$-based nanocomposites has a high effect on the degradation of aqueous solution pollutants.

Key words: aqueous solution, nanocomposites, $NiFe_2O_4$, photocatalyst, pollutants, systematic review

HIGHLIGHTS

- 454 studies were screened and using the inclusion and exclusion criteria, in total, 31 studies met our inclusion criteria.
- The percentage of photocatalytic degradation of pollutants by $NiFe_2O_4$-based nanoparticles was reported to be above 70%, and in some studies, the removal efficiency had reached 100%.

ABBREVIATIONS

PRISMA	Preferred Reporting Items for Systematic Reviews and Meta-Analyses
$NiFe_2O_4$-based nanoparticle	nanocomposites that have Nickel Ferrite in their structures
Photocatalyst	is a combination of two words: photo related to photon and catalyst, which is a substance altering the reaction rate in its presence.
MB	methylene blue dye
IBP	influence of persulfate on ibuprofen
RhB	rhodamine B
UDMH	unsymmetrical dimethylhydrazine
CP	chlorpyrifos
AMP	ampicillin
EBT	Eriochrome Black T
SMX	sulfamethoxazole
TC	tetracycline hydrochloride
MG	malachite green
IC	indigo carmine
NZF	$Ni_{0.5}Zn_{0.5}Fe_2O_4$ nanocomposites

INTRODUCTION

The rapid increase of populations causes the increase of non-degradable and toxic organic pollutants in water environments such as pharmaceuticals, dyes, aromatic compounds, acids etc (Naghizadeh *et al.* 2015; Azam *et al.* 2021; Xiao *et al.* 2021; Esmati *et al.* 2023). The rapid increase in industries has also increased water pollution and energy problems. Energy problems and water pollution are among the problems of the present age that threaten humans (Guo *et al.* 2021; Nawaz *et al.* 2022). Therefore, humans need a sustainable, efficient, and accessible technology to overcome the problem of water pollution. Considering the green and sustainable nature of sunlight, using solar energy with nanocomposites in water purification is a cost-effective and environmentally friendly method (Tang *et al.* 2019; Xie *et al.* 2020; Javadmoosavi *et al.* 2023). Nanoscience and nanotechnology can be used in various sciences such as water purification, textile, pharmaceutical, medicine, and printing, as well as today in the environment in order to remove many pollutants (Naghizadeh *et al.* 2013; Ren *et al.* 2019; Shams *et al.* 2019; Derakhshani *et al.* 2023). So far, a lot of research has been done on the synthesis of different nanomaterials and their application in different fields (Mousavi & Habibi-Yangjeh 2016; Mousavi-Kamazani *et al.* 2016; Ghoreishi *et al.* 2018; Shirzadi-Ahodashti *et al.* 2020b; Gholami *et al.* 2023). Nanocomposites with diameters between 1 and 100 nm have improved properties such as uniform size distribution, small size, high surface-to-volume ratio, high adsorption capacity, porosity, and various potential roles in catalytic and biological activities. For these reasons, nanocomposites have recently been synthesized and widely used in the removal of various pollutants from aqueous solutions (Khan *et al.* 2016; Akbari *et al.* 2019; Shams *et al.* 2019). Today, extensive efforts have been made to investigate the efficiency of spinel ferrites (MFe_2O_4) due to their unique physical and chemical properties (Polshettiwar *et al.* 2011; Jiang *et al.* 2020). In the past decades, various advanced methods have been used to synthesize different spinel ferrites, including the co-precipitation method, hydrothermal method, sol–gel method, mechanical alloying, solution thermal method, electrochemical synthesis, and chemical solution deposition method (Yan *et al.* 2013; Naghizadeh *et al.* 2017). Nowadays, Nickel ferrite ($NiFe_2O_4$) is known as an important spinel ferrite and has been studied in various fields due to its chemical stability and mechanical hardness. Today, composites derived from $NiFe_2O_4$ are used as photocatalysts for the decomposition of various pollutants in aqueous solutions (Hossein Panahi *et al.* 2020; Wang *et al.* 2022). Magnetic semiconductor photocatalysts are used in various environmental fields, including water and wastewater treatment, due to their high optical activity, non-toxicity, low cost, easy application in various environmental conditions, complete mineralization of pollutants, and chemical and thermal stability (Eslami *et al.* 2016; Ge *et al.* 2021; Sanadi *et al.* 2021; Derakhshani *et al.* 2022). Photocatalysts are materials that create a pair of electron holes on their surface as a result of sunlight or artificial light (such as UV light) so that the free radicals produced from this process have high oxidizing properties to destroy pollutants (Kamani *et al.* 2018; Asadzadeh Patehkhor *et al.* 2021). Photocatalysts actually provide the necessary conditions to carry out these reactions, but do not directly interfere with oxidation–reduction reactions. The obvious feature of a semiconductor photocatalyst is having capacitive and conductive bands. The space between these two bands is called the band gap (Bora & Dutta 2014; Shirzadi-Ahodashti *et al.* 2020a). The operation of a semiconductor photocatalyst is initiated by the irradiation of natural or artificial light on its surface. During light irradiation, due to the absorption of photons with energy equal to or greater than the energy of the photocatalytic band gap, the electrons of the capacitive band are excited and transferred from this band to the conduction band, and as a result of this transfer, the holes are simultaneously formed in capacitive bands. The lifetime of the electron–hole pair is only a few nanoseconds. But this short time is enough to carry out oxidation/reduction reactions in a solution containing a semiconductor. The created holes have a very high oxidation potential so that they are sufficient to produce hydroxyl radicals from water molecules and hydroxide ions adsorbed on the photocatalyst surface. The generated electrons react with the absorbed oxygen molecule and reduce it to superoxide radical. The superoxide radical produced reacts with a proton to form peroxide radicals. Hydrogen peroxide can also act as an electron acceptor and generate additional hydroxyl radicals (Safari *et al.* 2014; Shirzadi-Ahodashti *et al.* 2020b). So far, a complete systematic analysis has not yet been published to investigate the photocatalytic decomposition of pollutants by $NiFe_2O_4$-based nanocomposites in aqueous solutions. Therefore, in this study, our aim was to systematically review all research studies on the photocatalytic decomposition of pollutants by $NiFe_2O_4$-based nanocomposites and to evaluate the laboratory conditions and results of these studies.

METHODS

The present review research study was followed PRISMA (Preferred Reporting Items for Systematic Reviews and Meta-Analyses) guidelines (http://www.prisma-statement.org/).

Inclusion criteria

We included all the original studies in English that investigated the photocatalytic degradation of pollutants in aqueous solutions using $NiFe_2O_4$-based nanocomposites. In all the studies reviewed in this research, all the pollutants in water that were degraded by photocatalytic method by $NiFe_2O_4$-based nanocomposites were investigated.

Search strategy

The present study was a systematic review that was conducted by searching PubMed, Web of Science and Scopus databases until March 2022. The language of the searched articles was English. The search strategy in this systematic review is shown in Table 1. The following keywords were considered during the search:

Photodegradation, Photolysis, Photocatalysis, Photocatalytic, Photocatalyst, 'Photochemical processes', Nanoparticles, Nanocomposite, Nanoparticle, 'Nanocrystalline Materials', 'Nanocrystalline Material', Nanocrystals, Nanocrystal, $NiFe_2O_4$, 'Nickel ferrite', Water, 'aqueous solution'.

Data extraction

Data and information extracted from studies that were eligible for inclusion in this systematic review included the following:

(I) authors, (II) year of publication, (III) catalyst type and size, (IV) methods of synthesis, (V) type of pollutant, (VI) optimum pH, (VII) optimum initial concentration of pollutant, (VIII) optimum catalyst concentration, (IX) optimum time, (X) irradiation, (XI) removal efficiency.

Other important parameters included antibacterial performance of the photocatalyst, effect of interference and reusability of the photocatalyst, regeneration and reusability of the photocatalyst, effect of $NiFe_2O_4$ content in nanocomposite, effect of different catalysts on the degradation of methylene blue (MB), effect of H_2O_2 in the photocatalysis process, the effect of UV light intensity, effects of the initial oxalic $C(H_2C_2O_4)$ concentration, sonophotocatalysis with variable ultrasonic power intensities, influence of ultrasonic power and frequency, influence of persulfate on ibuprofen (IBP) mineralization, the effect of US frequency.

Synthesis method

We conducted a systematic review and since the data were heterogeneous, we did not perform any specific analysis and the data were reported as a narrative.

RESULTS AND DISCUSSION

After searching the databases, 454 articles were identified. From these articles, 54 were duplicates and were deleted. From the 400 remaining articles, 348 articles were excluded according to their title and abstract. Then from the 52 remaining articles, after reading the full text, 21 were excluded because they did not include the required outcome. Finally, 31 articles were included (Figure 1).

Table 1 | The search strategy in this systematic review

1	(((((((Nanoparticles[Title/Abstract]) OR (Nanocomposite[Title/Abstract])) OR (Nanoparticle[Title/Abstract])) OR ('Nanocrystalline Materials'[Title/Abstract])) OR ('Nanocrystalline Material'[Title/Abstract])) OR (Nanocrystals[Title/Abstract])) OR (Nanocrystal[Title/Abstract])) OR (Nanoparticles[MeSH Terms])
2	(($NiFe_2O_4$[Title/Abstract]) OR ('Nickel ferrite' [Title/Abstract]))
3	((((((Photolysis[MeSH Terms]) OR ('photochemical processes' [Title/Abstract])) OR (photocatalyst[Title/Abstract])) OR (photocatalytic[Title/Abstract])) OR (photocatalysis[Title/Abstract])) OR (Photolysis[Title/Abstract])) OR (Photodegradation[Title/Abstract])
4	((Water[Title/Abstract]) OR ('aqueous solution' [Title/Abstract])) OR (water[MeSH Terms])
5	#1 AND #2
6	#5 AND #3
7	#6 AND #4

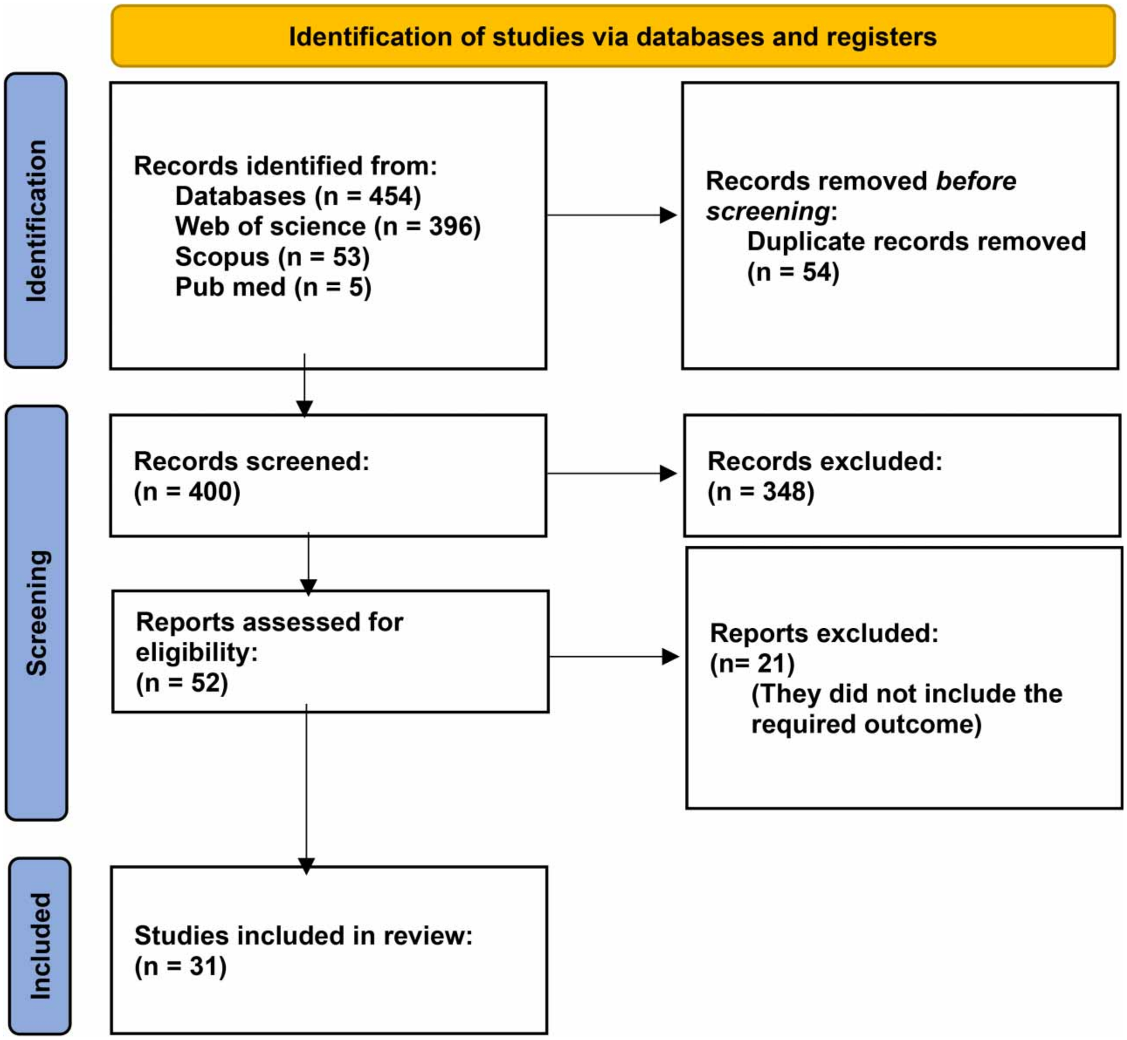

Figure 1 | Identification of studies via databases and registers.

Among the reviewed articles, the most recent article selected for systematic review was published in 2022 and the oldest was published in 2012. All investigated articles were in English. The studies were conducted in South Korea, India, Iran, Turkey, Philippines, Taiwan, United States of America, China, Indonesia, Saudi Arabia, Yemen, Sudan, and South Africa.

In most studies, optimum initial concentration of pollutants, optimum catalyst concentration, optimum pH and optimum time were investigated. In all these studies, nanocomposites based on $NiFe_2O_4$ were used, including: $Ag/AgBr/NiFe_2O_4$ (Ge *et al.* 2017), Ag–doped $Ni_{0.5}Zn_{0.5}Fe_2O_4$ (Mustafa & Oladipo 2021), $CdS–NiFe_2O_4/rGO$ (Bagherzadeh *et al.* 2018), ZIF-8/$NiFe_2O_4$ (Faraji *et al.* 2021), $GO/NiFe_2O_4/TiO_2$ (Lu *et al.* 2021), $NiFe_2O_4$ (Liu *et al.* 2012; Kazemi *et al.* 2018; Guo & Wang 2019; Nadumane *et al.* 2019; Vijay *et al.* 2019; Nawaz *et al.* 2020; Hariani *et al.* 2021), $NiFe_2O_4$:Mg^{2+} (Nadumane *et al.* 2019), cysteine modified graphene oxide@nickelferrite@titanium dioxide (Anirudhan *et al.* 2021), Pectin- $NiFe_2O_4$ (Gupta *et al.* 2020), $NiFe_2O_4/ZnO$ (Moradi *et al.* 2018; Yeganeh *et al.* 2020), $PANI/Ag_3PO_4/NiFe_2O_4$ (Chen *et al.* 2019a), $NiAl_xFe_{2-x}O_4$ ($x = 0–0.7$) (Naik *et al.* 2018), MWCNTs-$CuNiFe_2O_4$ (Al-Musawi *et al.* 2021), CdS nanorods/$NiFe_2O_4$/NaX zeolite (Sadeghi *et al.* 2020), Z-scheme APO/MOF/NFO (Zhou *et al.* 2018), $NiFe_2O_4$/T/GOx (Atacan *et al.* 2019), $NiFe_2O_4$@GO (Bayantong *et al.* 2021), $NiFe_2O_4$-rice husk char (RHC) (Han *et al.* 2018), NiFe-CNT (Nawaz *et al.* 2020), $NiFe_2O_4$/C yolk-shell (Chen *et al.* 2019b), Chitosan-Ascorbic Acid@$NiFe_2O_4$ (CTAS@NIFE) (Hasan *et al.* 2020), $TiO_{2-x}/NiFe_2O_4$ (Wu 2020), $NiFe_2O_4$–SQD (NF–SQDs) (Babu *et al.* 2021), MWCNT–$CuNiFe_2O_4$ (Al-Musawi *et al.* 2022), $NiFe_2O_4$/MWCNTs/ZnO (Hezam *et al.* 2020), (($NiFe_2O_4$-SiO_2), ($NiFe_2O_4$-TiO_2), ($NiFe_2O_4$-SiO_2-TiO_2) and TiO_2) (Ojemaye *et al.* 2017).

Different pollutants in aqueous solutions were degraded by using these nanocomposites. In nine studies the pollutant investigated was methylene blue (Bagherzadeh *et al.* 2018; Han *et al.* 2018; Kazemi *et al.* 2018; Guo & Wang 2019; Gupta *et al.* 2020; Hezam *et al.* 2020; Sadeghi *et al.* 2020; Bayantong *et al.* 2021; Faraji *et al.* 2021). Other pollutants included Rhodamine B (RhB) (Liu *et al.* 2012; Ge *et al.* 2017; Zhou *et al.* 2018; Chen *et al.* 2019a; Sadeghi *et al.* 2020), Metronidazole antibiotic (Mustafa & Oladipo 2021), Unsymmetrical dimethylhydrazine (UDMH) (Lu *et al.* 2021), (IC dye and Phenol) (Nadumane *et al.* 2019), Chlorpyrifos (CP) (Anirudhan *et al.* 2021), Remazol Black 5 (Gupta *et al.* 2020), Coomassie blue G-250 dye (Yeganeh *et al.* 2020), Methyl orange (MO) dyes (Chen *et al.* 2019a; Sadeghi *et al.* 2020), (blue 129 dye and reactive blue 21 dye) (Moradi *et al.* 2018), Rose bengal (RB) dye (Naik *et al.* 2018), Ampicillin (AMP) (Al-Musawi *et al.* 2021), Eriochrome Black T (EBT) (Sadeghi *et al.* 2020), Indigo Carmine (IC) (Atacan *et al.* 2019), Sulfamethoxazole (SMX) (Nawaz *et al.* 2020), Irgalite violet dye (Vijay *et al.* 2019), Tetracycline hydrochloride (TC) (Chen *et al.* 2019b), Malachite green (MG) (Hasan *et al.* 2020), ibuprofen (IBP) (Wu 2020), Congo red (Hariani *et al.* 2021), Tetracycline (TC) (Babu *et al.* 2021), Acid blue 113 dye (Al-Musawi *et al.* 2022), and Cr(VI) (Ojemaye *et al.* 2017).

The removal efficiency in most studies shows that $NiFe_2O_4$-based nanocomposites can remove pollutants from aqueous solutions by photocatalytic degradation process with a high percentage.

Influence of pH on photocatalytic activity of $NiFe_2O_4$-based nanocomposites

Table 2 also shows the experimental conditions and the investigated variables used in the included studies for the degradation of environmental pollutants from aqueous solutions by photocatalytic process using $NiFe_2O_4$-based nanocomposites. pH is one of the most important factors in the photocatalytic degradation process (Li *et al.* 2016). The optimum pH for the photocatalytic degradation of pollutants by $NiFe_2O_4$ was found to be equal to 2 based on two studies (Ojemaye *et al.* 2017; Han *et al.* 2018), equal to 2.5 in one study (Gupta *et al.* 2020), equal to 3 in five studies (Liu *et al.* 2012; Nadumane *et al.* 2019; Vijay *et al.* 2019; Nawaz *et al.* 2020; Yeganeh *et al.* 2020; Mustafa & Oladipo 2021), equal to 5 in four studies (Nawaz *et al.* 2020; Al-Musawi *et al.* 2021; Hariani *et al.* 2021; Al-Musawi *et al.* 2022), equal to 6 in one study (Wu 2020), equal to 6.5 in one study (Atacan *et al.* 2019), from 7 to 8 in seven studies (Bagherzadeh *et al.* 2018; Kazemi *et al.* 2018; Naik *et al.* 2018; Chen *et al.* 2019b; Guo & Wang 2019; Hasan *et al.* 2020; Anirudhan *et al.* 2021), equal to 6.8 in one study (Chen *et al.* 2019a), equal to 9 in two studies (Faraji *et al.* 2021; Lu *et al.* 2021), equal to 10 in two studies (Ge *et al.* 2017; Bayantong *et al.* 2021), in one study 11.5 (Hezam *et al.* 2020), and not reported in four studies (Moradi *et al.* 2018; Zhou *et al.* 2018; Sadeghi *et al.* 2020; Babu *et al.* 2021).

According to the results extracted in the previous studies and investigated in this study, the optimal pH was mentioned in different ranges, because the types of pollutant and their surface charges were different. Considering that photocatalytic processes are usually carried out on the surface of catalysts, the surface electric charge of different catalysts may be positive or negative depending on the catalyst components and surface functional groups. In photocatalytic processes, pHzpc plays a significant role, because in pHzpc, the positive and negative electric charges on the catalyst surface are balanced. At $pH > pHzpc$, the dominant electrical charge on the catalyst surface is negative due to excess OH ions, and at $pH < pHzpc$, the dominant electrical charge on the catalyst surface becomes positive due to H+ ions (Moein *et al.* 2020; Mohammadi *et al.* 2022).

For example, the results of Bayantong *et al.*'s study showed that the decolorization of methylene blue by $NiFe_2O_4$@GO photocatalytic nanocomposite is enhanced under alkaline conditions because methylene blue is a cationic organic dye (Bayantong *et al.* 2021). On the other hand, $NiFe_2O_4$@GO nanocomposite has a negative charge when $pH > pHzpc$ (Perreault *et al.* 2015). As a result, the surface charge of the nanocomposite and the dye are opposite in alkaline conditions, which causes the dye to adsorb on the surface of the nanocomposite and increase its degradation (Bayantong *et al.* 2021).

The results of another study conducted by Nadumane *et al.* showed that the highest efficiency for phenol occurred at $pH = 3$. Their reasoning was that in addition to OH° radicals produced by photofenton activities, at lower pH, hydrogen ions react to produce OH° radicals to degrade phenol. But in alkaline conditions, the hydroxyl ions in the solution are highly concentrated, which makes the sunlight not reach the surface of the photocatalyst, and as a result, the rate of decomposition decreases (Nadumane *et al.* 2019).

Influence of initial pollutants concentration on photocatalytic activity of $NiFe_2O_4$-based nanocomposites

The initial concentration of the desired pollutant in the water environment is one of the important parameters that affects the removal efficiency in the photocatalytic purification process (Darvishi Cheshmeh Soltani *et al.* 2016). In most of the studies

Table 2 | The main investigated parameters in the photocatalytic degradation of pollutants by $NiFe_2O_4$-based nanocomposites

					Optimum monitored parameters						
No.	**Nanocatalyst**	**Size**	**Synthesis methods**	**Pollutant**	**pH**	**Pollutant concentration**	**Catalyst concentration**	**Time**	**Irradiation method**	**Removal efficiency**	**References**
1	$Ag/AgBr/NiFe_2O_4$	50–150 nm	Hydrothermal	Rhodamine B (RhB)	10	10 mg/L	–	60 min	visible light irradiation	–	Ge *et al.* (2017)
2	Ag–doped $Ni_{0.5}Zn_{0.5}Fe_2O_4$	< 5 μm	co-precipitation	metronidazole antibiotic	3	50 mg/L	10 mg per 25 mL	360 min	UV	–	Mustafa & Oladipo (2021)
3	$CdS–NiFe_2O_4/rGO$	20–40 nm	hydrothermal	methylene blue (MB)	7	10 mg/L	0.4 g/L	120 min	visible light	–	Bagherzadeh *et al.* (2018)
4	$ZIF-8/NiFe_2O_4$	–	Hydrothermal and green method	methylene blue (MB)	9	5 mg/L	0.05 g	120 min	visible-light	94%	Faraji *et al.* (2021)
5	$GO/NiFe_2O_4/TiO_2$	Length: 1.65 μm diameter: 60–120 nm	TiO2 NRAs: hydrothermal NiFe2O4/TiO2 NRAs: dipping and annealing GO : modified Hummers' method	unsymmetrical dimethylhydrazine (UDMH)	9	20 mg/L	–	90 min	visible light	73.1%	Lu *et al.* (2021)
6	$NiFe_2O_4$ $NiFe_2O_4$: Mg2 +	62.2–9.28 μm 0.46–8.33 μm	modified green sol–gel route	IC dye and Phenol	3	20 ppm	40 mg	120 min	Sunlight irradiation	–	Nadumane *et al.* (2019)
7	Cysteine modified Graphene oxide@nickelferrite@titanium dioxide	–	–	chlorpyrifos (CP)	7	10 mg/L	2 g/L	1 h	visible light irradiation	99.5%	Anirudhan *et al.* (2021)
8	Pectin- $NiFe_2O_4$	15–20 nm	hydrothermal	Methylene blue & Remazol Black 5	2.5	0.05 mM	0.5 g/L	Methylene blue: 35 min Remazol Black 5: 30 min	visible light	Methylene blue: 99.57% Remazol Black 5: 99.68%	Gupta *et al.* (2020)
9	$NiFe_2O_4/ZnO$:ZnO $NiFe_2O_4$	: 48–52 nm 25–31 nm	solidification and calcination methods	Coomassie blue G-250 dye	3	–	0.1 g	60 min	Visible and UV light	–	Yeganeh *et al.* (2020)
10	$PANI/Ag_3PO_4/NiFe_2O_4$		Precipitation hydrothermal method	Rhodamine B (RhB) and methyl orange (MO) dyes	6.8	Optimum initial concentration of RhB dye: 10 mg/L	1 g/L	30 min	visible-light	RhB: 100% MO: 94.97%	Chen *et al.* (2019a)
11	$NiFe_2O_4$	155–185 nm	solvothermal process	Methylene Blue (MB)	7	0.03 g/L	0.2 g/L	50 min	UV	98.5%	Guo & Wang (2019)
12	$NiFe_2O_4$@ ZnO	35–45 nm	green sol–gel method	blue 129 dye and reactive blue 21 dye	–	2 mg/L	0.05 g for DB129 and 0.07 g for RB21	60 min	visible light	blue 129 dye: 98% reactive blue 21 dye: 96%	Moradi *et al.* (2018)
13	$NiAl_xFe_{2-x}O_4$ (x = 0–0.7)	19–38 nm	sol–gel auto-combustion method	rose bengal (RB) dye	8	5 ppm/100 mL	40 mg/100 ml	150 min	visible light	99.8%	Naik *et al.* (2018)

(*Continued.*)

Table 2 | Continued

No.	Nanocatalyst	Size	Synthesis methods	Pollutant	Optimum monitored parameters: pH	Pollutant concentration	Catalyst concentration	Time	Irradiation method	Removal efficiency	References
14	MWCNTs-$CuNiFe_2O_4$	2–14 nm	Co-precipitation	Ampicillin (AMP)	5	25 mg/L	0.5 g/L	60 min	UV	100%	Al-Musawi *et al.* (2021)
15	CdS nanorods/$NiFe_2O_4$/NaX zeolite: ($NiFe_2O_4$)	15 nm	simple ultrasound-assisted solvothermal method	Methylene Blue (MB), Eriochrome Black T (EBT), Rhodamine B (RhB) and Methyl Orange (MO)	_	25 mg/L	50 mg	60 min	Ultrasonic	MB: 100% RhB: 97.4% EBT: 90% MO: 85.3%	Sadeghi *et al.* (2020)
16	Z-scheme APO/MOF/NFO	–	precipitation method	Rhodamine B (RhB)	_	5 mg/L	0.4 g/L	_	visible-light irradiation	_	Zhou *et al.* (2018)
17	$NiFe_2O_4$/T/GOx	–	solvothermal method	Indigo Carmine (IC)	6.5	10 mg/L	_	90 min	Bio-Fenton process & UV lamp	Bio-Fenton process: 37.6% UV lamp: 98.6%	Atacan *et al.* (2019)
18	$NiFe_2O_4$	20–25 nm	_	Methylene Blue (MB)	7.81	20 mg/L	22.35 mg	67 min	UV light irradiation	95.8%	Kazemi *et al.* (2018)
19	$NiFe_2O_4$@GO	7.76 nm	solution combustion synthesis route	Methylene Blue (MB)	10	0.04 mM	0.5 g/L	120 min	UV light irradiation	_	Bayantong *et al.* (2021)
20	$NiFe_2O_4$-rice husk char (RHC)	–	simple soft chemical way	Methylene Blue (MB)	2	10 mg/L	_	_	Visible-Light Irradiation	_	Han *et al.* (2018)
21	$NiFe_2O_4$-	10 nm	Hydrothermal method	Rhodamine B (RhB)	3	10 mg/L	0.2 g/L	30 min	UV	_	Liu *et al.* (2012)
22	$NiFe_2O_4$ & NiFe-CNT		one-step hydrothermal treatment	sulfamethoxazole (SMX)	5	5 ppm	0.025 g/L	2 h	ultraviolet (UV)-A & visible light	100%	Nawaz *et al.* (2020)
23	$NiFe_2O_4$		Co-precipitation method	Irgalite violet dye	3	400 ppm	0.2 g	60 min	sunlight	99%	Vijay *et al.* (2019)
24	$NiFe_2O_4$/C yolk-shell-	200–400 nm	hydrothermal deposition method	tetracycline hydrochloride (TC)	7.5	_	0.3 g/L	60 min	visible light irradiation	97.25%	Chen *et al.* (2019b)
25	Chitosan-Ascorbic Acid@$NiFe_2O_4$ (CTAS@NIFE)-	5.15 nm	chemical co-precipitation method	malachite green (MG)	8	70 mg/L	_	90 min	visible light irradiation coupled with ultrasonic waves	99%	Hasan *et al.* (2020)
26	TiO_{2-x}/$NiFe_2O_4$	–	Consecutive sol–gel processes	ibuprofen (IBP)	6	10 mg/L	0.7 g/L	100 min	ultrasonic irradiation	96.70%	Wu (2020)
27	$NiFe_2O_4$:	10–40 nm	solution combustion method	Congo red	5	100 mg/L	_	60 min	Visible light	96.80%	Hariani *et al.* (2021)
28	$NiFe_2O_4$–SQD (NF–SQDs)	54.37 nm	hydrothermal synthesis	tetracycline (TC)	_	40 mg/L	15 mg	70 min	sunlight irradiation	98%	Babu *et al.* (2021)
29	MWCNT–$CuNiFe_2O_4$	–	Co-precipitation	acid blue 113 dye	5	50 mg/L	0.6 g/L	30 min	UV	100%	

(*Continued*.)

Table 2 | Continued

No.	Nanocatalyst	Size	Synthesis methods	Pollutant	Optimum monitored parameters: pH	Pollutant concentration	Catalyst concentration	Time	Irradiation method	Removal efficiency	References
											Al-Musawi *et al.* (2022)
30	$NiFe_2O_4$/MWCNTs/ZnO	–	hydrothermal and the co-precipitation methods	Methylene Blue (MB) dye	11.5	20 mg/L	1 g/L	300 min	visible light	73.02%	Hezam *et al.* (2020)
31	($NiFe_2O_4$-SiO_2), ($NiFe_2O_4$-TiO_2), ($NiFe_2O_4$-SiO_2-TiO_2) and TiO_2	–	Co-precipitation and sol–gel methods	Cr(VI)	2	_	200 mg	TiO_2: 240 min ($NiFe_2O_4$-SiO_2-TiO_2): 300 min ($NiFe_2O_4$-TiO_2): 300 min	UV irradiation	TiO_2: 96.7% ($NiFe_2O_4$-SiO_2-TiO_2): 96.50% ($NiFe_2O_4$-TiO_2): 60%	Ojemaye *et al.* (2017)

that investigated the effect of the initial concentration of the environmental pollutants, they concluded that the efficiency of the photocatalytic degradation process decreases with the increase of the initial concentration of the pollutant.

The reason for the decrease in efficiency with the increase in the initial concentration of the target pollutant is that at lower concentrations there is more surface on the catalyst to adsorb the pollutant. But with the increase of pollutant concentration, more molecules are adsorbed on the active surface groups of catalyst nanocomposites and therefore reduce the available reaction sites (Wang *et al.* 2012; Khodadadi *et al.* 2020).

On the other hand, the concentration of free radicals produced in all solutions is equal to the different concentration of the pollutant; therefore, a solution with a low pollutant concentration with the same amount of hydroxyl radical will have a higher decomposition rate than a solution with a higher concentration (Wang *et al.* 2012).

Influence of catalyst dose on photocatalytic activity of $NiFe_2O_4$-based nanocomposites

The optimal photocatalytic nanocomposites dose in aqueous solution is one of the most important parameters on the efficiency of photocatalytic processes (Kamani *et al.* 2021). The results of the investigated studies showed that at low doses of photocatalyst, the degradation efficiency increases with the increase of the catalyst dose. The reason is the increase in the number of active sites on the surface of the nanocatalyst. However, very high doses of photocatalyst increase the turbidity in the solution. This turbidity prevents the penetration of light into the solution and increases the scattering of light in the solution, which ultimately leads to a weak light reaction and a decrease in the efficiency of the degradation of impurities (Pei & Leung 2013).

However, in general, the increase or decrease of the performance of the photocatalyst process depends on the dosage range of the nanocatalyst. If the selected range of catalyst dosage is low enough not to cause additional turbidity, the performance of photocatalytic degradation will increase with increasing nanocatalyst dosage. But if the dosage range of the selected catalyst is wide and includes high dosages that cause turbidity, usually by increasing the catalyst dosage beyond a certain limit, the degradation performance decreases due to the prevention of proper radiation and lack of light penetration (Kamranifar *et al.* 2019; Derakhshani *et al.* 2022).

Influence of contact time on photocatalytic activity of $NiFe_2O_4$-based nanocomposites

Another parameter that affects the photocatalytic decomposition of pollutants is the appropriate contact time of the pollutant with the nanocatalyst, which has been investigated in some studies. The results of these studies showed that in the early stages of degradation, the amount of contact between the nanocatalyst and the pollutant is higher and the number of holes on the surface of the nanocatalyst is higher. With the gradual occupation of these holes and places by the pollutant, the amount of destruction decreases compared to the initial stages, and after a certain period of time, the amount of destruction reaches a constant value and may decrease after that (Oskoei *et al.* 2016). In a study conducted by Kazemi *et al.*, the effect of time on the decomposition of methylene blue was investigated for 30–150 min. The results of their study showed that the rate of photocatalytic degradation of methylene dye increased with increasing contact time, but after 60 min, the degradation was almost constant (Kazemi *et al.* 2018).

As is clear from Table 3, in some of the reviewed studies, other parameters have been investigated in addition to the parameters in Table 2, some of which we will explain below:

Antibacterial performance of $NiFe_2O_4$-based nanocomposites

Antibacterial agents cause rapid recovery of bacterial infections and also reduce the possibility of bacterial resistance to drugs, which is why antibacterial agents are widely used in the medical field (Hanif *et al.* 2019). Mustafa *et al.* investigated the photocatalytic degradation of metronidazole by Ag-doped $Ni_{0.5}Zn_{0.5}Fe_2O_4$ nanocomposites and also the antibacterial activity of Ag-d-NZF against *Escherichia coli* and Staphylococcus aureus. The results showed that Ag-d-NZF has more antibacterial activity on *E. coli* than *Staphylococcus aureus* strains, which is probably due to changes in the structure and composition of the cell membrane (Mustafa & Oladipo 2021).

Stability and reuse of $NiFe_2O_4$-based nanocomposites

For the use of synthesized nanocatalysts in industry, it is important to determine the reusability of consumed nanocatalysts in order to reduce costs and availability of nanocatalysts for photocatalytic processes and environmental safety (Ojemaye *et al.* 2017).

Table 3 | Other investigated parameters in the photocatalytic degradation of pollutants by $NiFe_2O_4$-based nanocomposites

Other monitored parameters	Reference
Antibacterial performance of Ag–d-NZF: Ag–doped $Ni_{0.5}Zn_{0.5}Fe_2O_4$ had higher antibacterial activity on *E. coli* than *S. aureus* strains.	Mustafa & Oladipo (2021)
Effect of interference and reusability of Ag–d-NZF: The lowest degradation was recorded in the presence of NO_3 due to its quenching effect. The degradation efficiency of Ag-d-NZF decreased to ~71% in the second reuse step and decreased to ~57% in the fifth reuse step.	
Stability of the photocatalyst: There was no significant decrease in photocatalyst activity for six cycles, and the photocatalyst could be reused for more than six photocatalytic cycles.	Bagherzadeh *et al.* (2018)
Effect of $NiFe_2O_4$ content in nanocomposite: The highest photocatalytic activity for methylene blue (MB) degradation was for Z/NFO-30 sample compared to Z/NFO-10, Z/NFO-50 and Z/NFO-70.	Faraji *et al.* (2021)
Effect of different catalysts on the degradation of methylene blue (MB): Among ZIF-8, $NiFe_2O_4$ and Z/NFO-30 composites, Z/NFO-30 nanocomposite demonstrated the highest methylene blue (MB) removal efficiency (94% after 120 min).	
Regeneration and reusability of the photocatalyst: The results showed that the photocatalysts are stable and usable for several times.	
Effect of H_2O_2 in photocatalysis process: The degradation rate gradually increased up to 6 mM for IC dye and then decreased with increasing dose. For phenol, the rate of degradation increased up to 5 mM and then decreased with increasing dose	Nadumane *et al.* (2019)
Investigating the stability and reuse of nanocomposites: The irradiation-separation-washing process can be repeated several times, while maintaining the high photocatalytic activity of nanocomposites for IC dye and phenol degradation.	
The influence of $H_2C_2O_4$ concentration: The results showed that the rate of methylene blue decolorization increases with increasing the dose of $H_2C_2O_4$ from 0 to 0.06 g/L.	Guo & Wang (2019)
The effect of H_2O_2 dosage on the MB degradation: The results showed that the degradation of methylene blue increased with increasing the dose of H_2O_2 from 0 to 5 mM and the degradation rate was over 98.5%.	
Effect of visible light irradiation on removal of dyes: The results showed that no degradation was observed in the presence of visible light and without the addition of a catalyst. Also, dye degradation in the presence of magnetic nanocomposite in dark conditions was 39% for DB129 and 25% for RB21. But the dye degradation in the presence of visible light and magnetic nanocomposite for DB129 and RB21 was above 96% in 60 min.	Moradi *et al.* (2018)
Reuse of the photocatalyst: The results of this study showed that the photocatalytic activity of magnetic nanocomposite in color degradation does not decrease after five reuses. As a result, this catalyst is economical and stable in removing pollutants.	
The effect of UV light intensity: From the results of this study, it can be seen that the degradation rate of ampicillin increases with the increase of light intensity from 8 to 36 W.	Al-Musawi *et al.* (2021)
Stability study: To evaluate the recyclability of the photocatalyst, ampicillin photodegradation experiments were performed in eight consecutive reaction cycles under the same conditions. The results showed that the degradation rate of ampicillin decreased slowly from 100% in the third round to 93.72% in the eighth round.	
H_2O_2 volume: The rate constant initially increased with increasing volume of H_2O_2 up to 4 mL and then decreased.	Han *et al.* (2018)
Cycle performance: The degradation efficiency was unchanged after five recycling cycles of nanocomposites.	
Effects of the initial oxalic $C(H_2C_2O_4)$ concentration: By increasing the concentration of oxalic acid from 0.1 to 1.0 mM, the decomposition rate of Rhodamine B increased, and then at concentrations higher than 1.0 mM, the decomposition rate remained constant.	Liu *et al.* (2012)

(*Continued.*)

Table 3 | Continued

Other monitored parameters	Reference
Stability and reuse of catalyst: The results showed that the used catalyst is stable and recoverable because the decolorization ratio in all seven steps was more than 90.0%.	
H_2O_2 concentration: The optimal concentration of H_2O_2 for the degradation of sulfamethoxazole was found to be 1 μL/mL. At concentrations higher than 1 μL/mL, incomplete removal of SMX from the reaction solution occurred.	Nawaz *et al.* (2020)
Reusability and stability of the NiFe-CNT composite: The results showed that the degradation efficiency by the NiFe-CNT composite decreased by approximately 20% after five cycles.	
The effect of H_2O_2 concentration on the tetracycline hydrochloride (TC) degradation: The degradation efficiency of TC increased greatly as the initial volume of H_2O_2 increased from 0 to 0.1 mL, then decreased with further addition to 1 mL.	Chen *et al.* (2019b)
Sonophotocatalysis with Variable Ultrasonic Power Intensities: The results showed that the percentage of malachite green (MG) degradation increased with increasing density of ultrasonic power.	Hasan *et al.* (2020)
Influence of ultrasonic power and frequency: In this study, the degradation percentage of ibuprofen (IBP) increased with increasing ultrasonic power.	Wu (2020)
Influence of persulfate on ibuprofen (IBP) mineralization: The addition of PS to the sonocatalytic system increased the removal efficiency of ibuprofen (IBP) and the detoxification efficiency.	
Reusability and stability evaluation: In this study, the high recyclability of the sonocatalyst was reported, because the removal percentage of ibuprofen was 96.7% in the first use, and it slightly decreased in the sixth use and reached 95.8%.	
The effect of the intensity of UV light: The results showed that by increasing UV intensity from 8 to 36 W, acid blue 113 dye degradation efficiency at a reaction time of 25 min increased from 80.59 to 100%.	Al-Musawi *et al.* (2022)
The effect of US frequency: In this study by increasing the frequency from 20 to 35 kHz, the acid blue 113 dye degradation efficiency at a reaction time of 30 min increased from 86.49 to 99.06%.	
Regenerability and reusability study: The results showed that the photocatalyst materials can be regenerated for reuse and $NiFe_2O_4$-SiO_2-TiO_2 showed better reusability than $NiFe_2O_4$-TiO_2.	Ojemaye *et al.* (2017)

Moradi *et al.* investigated the reuse of $NiFe_2O_4$@ZnO nanocatalysts. They concluded that the photocatalytic activity of $NiFe_2O_4$@ZnO nanocomposite does not decrease in color degradation after five reuses. As a result, this catalyst is very stable and cost-effective in removal pollutants (Moradi *et al.* 2018). Nawaz *et al.* recycled the NiFe-CNT nanocomposite five times in order to investigate its stability and recyclability. The results showed that almost all the functional groups were present in the recycled photocatalytic materials and all the composite components were intact and stable (Nawaz *et al.* 2020).

Influence of H_2O_2 addition on pollutants degradation by $NiFe_2O_4$-based nanocomposites

H_2O_2 is used as an inorganic oxidant to increase the rate of photocatalytic reactions. Because hydrogen peroxide requires less energy than molecular oxygen to produce hydroxyl radicals, hydrogen peroxide is a better electron acceptor (Kim *et al.* 2013; Derakhshani *et al.* 2022).

The effect of H_2O_2 concentration on the degradation of sulfamethoxazole (SMX) was investigated by Nawaz *et al.* Based on the results obtained from their study, the optimal concentration of H_2O_2 for the degradation of SMX was found to be 1 μL/mL. At concentrations higher than 1 μL/mL, incomplete removal of SMX from the reaction solution occurred (Nawaz *et al.* 2020).

Chen *et al*. investigated the effect of H_2O_2 concentration on the degradation of TC. They concluded that the degradation efficiency of TC increased sharply as the initial volume of H_2O_2 increased from 0 to 0.1 mL, then decreased upon further addition to 1 mL.

The effect of UV light intensity on photocatalytic activity of $NiFe_2O_4$-based nanocomposites

In a study, Al-Musawi *et al.* investigated the effect of UV light intensity on the degradation efficiency of ampicillin (AMP) by MWCNTs-$CuNiFe_2O_4$ nanocomposites. From the results of this study, it can be seen that the degradation rate of ampicillin increases with the increase of light intensity from 8 to 36 W. Increasing the degradation rate of ampicillin may be related to the production of more protons, which are required to transfer electrons from the valence band to the conduction band to production more reactive species (Al-Musawi *et al.* 2021).

Other parameters investigated in studies for the photocatalytic degradation of pollutants by $NiFe_2O_4$-based are described in Table 3. In addition, advantages and disadvantages of $NiFe_2O_4$-based nanocomposites synthesis methods are shown in Table 4.

Challenges and future prospective

Advancement in the technology sector is increasing day by day due to the advancement of nanotechnology. It is expected that the use of nanostructures and nanomaterials will increase rapidly in the coming years, especially in water and wastewater treatment and removal of pollutants from the environment. Inadequate water resources and deterioration of their quality cause water scarcity, which adversely affects living organisms and the environment. The development of technological advancements, especially in the field of nanotechnology, may help to overcome these effects. Some nanomaterials are very toxic to humans and the environment. If these nanomaterials are used in water purification and their residues remain in the water, it leads to various poisonings. Therefore, researchers should focus on new techniques to standardize the measurement of hazardous effects of nanomaterials on human health.

The synthesis of nickel-based nanocomposites has often been associated with various challenges. These may mostly involve the problem of reduction of Ni(II) to Ni(0) at room temperature (Hossain *et al.* 2018). Only a few investigations are reported using nickel-based nanocomposites as adsorbents or photo catalysts in wastewater treatment. Plant extracts containing compounds that serve as reducing and capping agents in stabilizing the nanoparticles of Ni and NiO are to be identified in the

Table 4 | Advantages and disadvantages of synthesis methods of $NiFe_2O_4$-based nanocomposites

Synthesis methods	Advantages	Disadvantages
Hydrothermal method (Basavegowda & Baek 2021)	• High vapor pressures • Minimal loss of nanomaterials • Well controlled through liquid-phase or multiphase chemical reactions	• Use of expensive equipment • Use of high temperatures
Co-precipitation method (Entwistle *et al.* 2022)	• No solid waste • Effective and proved technologies • No daily use of chemicals	• Required trained person for maintenance and regeneration • Toxic liquid waste • Re-adjustment of pH may be necessary • Requires monitoring of breakthrough
Green method (Pal *et al.* 2022, Gholami *et al.* 2023)	• Cost-effective • Environmentally friendly • Low maintenance • Easy synthesis • Biocompatible • High stability • Easy available	• Uneven and irregular shape and size • Low yield • Less ideal quality of product • Practical difficulties in application
Sol–gel method (Bokov *et al.* 2021)	• Production of high-quality materials • Production of homogenous and high purity materials • Operating in lower temperature than conventional methods	• Long processing time • Difficult to avoid residual porosity and OH groups

available flora. Therefore green synthesis of nickel-based nanocomposites is a promising area for future research. Microbial mediated synthesis of nano-Ni and NiO are less investigated, and this is another vital aspect for research (Verma *et al.* 2021).

Photocatalytic decomposition of pollutants using nickel-based nanocomposites mainly depends on the type of pollutants, solution pH and concentration, catalysts and their composition, catalyst loading, solvent types, temperature and light intensity. While the advantages of using nickel nanocomposites as catalysts are emphasized, the disadvantages are not listed. It is hoped that in the future more emphasis will be placed on the use of nickel nanocomposites on a laboratory scale in the removal of pollutants. Also, the problems related to the residue of these nanocomposites in water, including their toxic properties on humans, should be investigated.

CONCLUSION

The comprehensive systematic review highlighted the photocatalytic degradation of pollutants using $NiFe_2O_4$-based nanocomposites in aqueous solution. In all the articles, the topic of photodegradation of pollutants using $NiFe_2O_4$-based nanocomposites was studied. The photocatalytic activity of the synthesized nanocomposite photocatalysts for degradation of various pollutants was also studied. The available literature reviewed here has shown an increasing interest in photocatalytic processes for the removal of pollutants by $NiFe_2O_4$-based nanocomposites from aqueous media in recent years. The most degraded pollutants in the studied research works were methylene blue dye and Rhodamine B with degradation efficiencies of 100%. Considering this variety, it can be mentioned that the photocatalytic process using $NiFe_2O_4$-based nanocomposites has been successful in breaking down aqueous solution pollutants.

ACKNOWLEDGEMENT

This article is part of the PhD thesis accepted in Birjand University of Medical Sciences, Iran coded 456905 and the side project accepted and financially supported by Research deputy of BUMS coded 2039. The authors are also grateful to the staff of the Medical Toxicology and Drug Abuse Research Center (MTDRC) for assisting in the analyses.

ETHICAL APPROVAL

This article does not contain any studies with human participants or animals performed by any of the authors.

CONSENT TO PUBLISH

All the authors mentioned in the manuscript have agreed to authorship, read, and approved the manuscript, and given consent for submission and subsequent publication of the manuscript.

AUTHORS CONTRIBUTIONS

All authors contributed to the study conception and design. Material preparation, data collection and analysis were performed by E.D. and A.N. The first draft of the manuscript was written by E.D. and all authors commented on previous versions of the manuscript. All authors read and approved the final manuscript.

FUNDING

This article is part of the PhD thesis accepted in Birjand University of Medical Sciences, Iran coded 456905 and the side project accepted and financially support in Research deputy of BUMS coded 6022.

DATA AVAILABILITY STATEMENT

All relevant data are included in the paper or its Supplementary Information.

CONFLICT OF INTEREST

The authors declare there is no conflict.

REFERENCES

Akbari, F., Khodadadi, M., Hossein Panahi, A. & Naghizadeh, A. 2019 Synthesis and characteristics of a novel $FeNi_3/SiO_2/TiO_2$ magnetic nanocomposites and its application in adsorption of humic acid from simulated wastewater: study of isotherms and kinetics. *Environmental Science and Pollution Research* **26**, 32385–32396.

Al-Musawi, T. J., Rajiv, P., Mengelizadeh, N., Arghavan, F. S. & Balarak, D. 2021 Photocatalytic efficiency of $CuNiFe_2O_4$ nanoparticles loaded on multi-walled carbon nanotubes as a novel photocatalyst for ampicillin degradation. *Journal of Molecular Liquids* **337**, 116470.

Al-Musawi, T. J., Mengelizadeh, N., Taghavi, M., Shehu, Z. & Balarak, D. 2022 Capability of copper-nickel ferrite nanoparticles loaded onto multi-walled carbon nanotubes to degrade acid blue 113 dye in the sonophotocatalytic treatment process. *Environmental Science and Pollution Research* **29**, 51703–51716.

Anirudhan, T. S., Manjusha, V. & Shainy, F. 2021 Magnetically retrievable cysteine modified graphene oxide@nickelferrite@titanium dioxide photocatalyst for the effective degradation of chlorpyrifos from aqueous solutions. *Environmental Technology & Innovation* **23**, 101633.

Asadzadeh Patehkhor, H., Fattahi, M. & Khosravi-Nikou, M. 2021 Synthesis and characterization of ternary chitosan–TiO_2–ZnO over graphene for photocatalytic degradation of tetracycline from pharmaceutical wastewater. *Scientific Reports* **11**, 24177.

Atacan, K., Guy, N., Cakar, S. & Ozacar, M. 2019 Efficiency of glucose oxidase immobilized on tannin modified $NiFe_2O_4$ nanoparticles on decolorization of dye in the Fenton and photo-biocatalytic processes. *Journal of Photochemistry and Photobiology A-Chemistry* **382**, 111935.

Azam, M., Liu, L. & Ahmad, N. 2021 Impact of institutional quality on environment and energy consumption: evidence from developing world. *Environment, Development and Sustainability* **23**, 1646–1667.

Babu, B., Koutavarapu, R., Shim, J., Kim, J. & Yoo, K. 2021 Improved sunlight-driven photocatalytic abatement of tetracycline and photoelectrocatalytic water oxidation by tin oxide quantum dots anchored on nickel ferrite nanoplates. *Journal of Electroanalytical Chemistry* **900**, 115699.

Bagherzadeh, M., Kaveh, R., Ozkar, S. & Akbayrak, S. 2018 Preparation and characterization of a new CdS-$NiFe_2O_4$/reduced graphene oxide photocatalyst and its use for degradation of methylene blue under visible light irradiation. *Research on Chemical Intermediates* **44**, 5953–5979.

Basavegowda, N. & Baek, K. H. 2021 Multimetallic nanoparticles as alternative antimicrobial agents: challenges and perspectives. *Molecules* **26**, 912.

Bayantong, A. R. B., Shih, Y. J., Dong, C. D., Garcia-Segura, S. & De Luna, M. D. G. 2021 Nickel ferrite nanoenabled graphene oxide ($NiFe_2O_4$@GO) as photoactive nanocomposites for water treatment. *Environmental Science and Pollution Research* **28**, 5472–5481.

Bokov, D., Turki Jalil, A., Chupradit, S., Suksatan, W. & Ansari, M. 2021 Nanomaterial by sol-gel method: synthesis and application. *Advances in Materials Science and Engineering* **2021**, 5102014.

Bora, T. & Dutta, J. 2014 Applications of nanotechnology in wastewater treatment—A review. *Journal of Nanoscience and Nanotechnology* **14**, 613–626.

Chen, Y. J., Zhu, P. F., Duan, M., Li, J., Ren, Z. H. & Wang, P. P. 2019a Fabrication of a magnetically separable and dual Z-scheme PANI/$Ag_3PO_4/NiFe_2O_4$ composite with enhanced visible-light photocatalytic activity for organic pollutant elimination. *Applied Surface Science* **486**, 198–211.

Chen, Z., Gao, Y. T., Mu, D. Z., Shi, H. F., Lou, D. W. & Liu, S. Y. 2019b Recyclable magnetic $NiFe_2O_4$/C yolk-shell nanospheres with excellent visible-light-Fenton degradation performance of tetracycline hydrochloride. *Dalton Transactions* **48**, 3038–3044.

Darvishi Cheshmeh Soltani, R., Safari, M. & Mashayekhi, M. 2016 Sonocatalyzed decolorization of synthetic textile wastewater using sonochemically synthesized MgO nanostructures. *Ultrasonics Sonochemistry* **30**, 123–131.

Derakhshani, E., Naghizadeh, A., Arabzozani, M. & Frakhondeh, T. 2022 A systematic review of photocatalytic degradation of humic acid in aqueous solution using nanoparticles. *Reviews on Environmental Health* https://doi.org/10.1515/reveh-2022-0046.

Derakhshani, E., Naghizadeh, A. & Mortazavi-Derazkola, S. 2023 Biosynthesis of MnFe(2)O(4)@TiO(2) magnetic nanocomposite using oleaster tree bark for efficient photocatalytic degradation of humic acid in aqueous solutions. *Environmental Science and Pollution Research* **30**, 3862–3871.

Entwistle, T., Sanchez-Perez, E., Murray, G., Anthonisamy, N. & Cussen, S. 2022 Co-precipitation synthesis of nickel-rich cathodes for Li-ion batteries. *Energy Reports* **8**, 67–73.

Eslami, A., Amini, M. M., Yazdanbakhsh, A. R., Mohseni-Bandpei, A., Safari, A. A. & Asadi, A. 2016 N,S co-doped TiO_2 nanoparticles and nanosheets in simulated solar light for photocatalytic degradation of non-steroidal anti-inflammatory drugs in water: a comparative study. *Journal of Chemical Technology & Biotechnology* **91**, 2693–2704.

Esmati, M., Allahresani, A. & Naghizadeh, A. 2023 Synthesis and characterization of Graphitic Carbon Nitride/Mesoporous Nano-Silica (g-C3N4/KCC-1) nanocomposite as a novel highly efficient and recyclable photocatalyst for degradation of antibiotic in aqueous solution. *Research on Chemical Intermediates* **47**, 1447–1469.

Faraji, A., Mehrdadi, N., Mahmoodi, N. M., Baghdadi, M. & Pardakhti, A. 2021 Enhanced photocatalytic activity by synergic action of ZIF-8 and $NiFe_2O_4$ under visible light irradiation. *Journal of Molecular Structure* **1223**, 129028.

Ge, M., Liu, M., Hu, X. & Li, Z. 2017 Magnetically separable Ag/AgBr/$NiFe_2O_4$ composite as a highly efficient visible light plasmonic photocatalyst. *Journal of Physics and Chemistry of Solids* **109**, 1–8.

Ge, T., Jiang, Z., Shen, L., Li, J., Lu, Z., Zhang, Y. & Wang, F. 2021 Synthesis and application of Fe_3O_4/$FeWO_4$ composite as an efficient and magnetically recoverable visible light-driven photocatalyst for the reduction of Cr(VI). *Separation and Purification Technology* **263**, 118401.
Gholami, M., Mortazavi-Derazkola, S. & Naghizadeh, A. 2023 Eco-friendly synthesis of CuO nanoparticles using Pulicaria gnaphalodes extract and biological and photocatalytic properties. *Biomass Conversion and Biorefinery*. https://doi.org/10.1007/s13399-023-04384-6.
Ghoreishi, S. M., Khalaj, A., Sabzevari, O., Badrzadeh, L., Mohammadzadeh, P., Mousavi Motlagh, S. S., Bitarafan-Rajabi, A. & Shafiee Ardestani, M. 2018 Technetium-99 m chelator-free radiolabeling of specific glutamine tumor imaging nanoprobe: in vitro and in vivo evaluations. *International Journal of Nanomedicine* **13**, 4671–4683.
Guo, X. J. & Wang, D. G. 2019 Photo-Fenton degradation of methylene blue by synergistic action of oxalic acid and hydrogen peroxide with NiFe2O4 hollow nanospheres catalyst. *Journal of Environmental Chemical Engineering* **7**, 102814.
Guo, S., Li, X., Li, J. & Wei, B. 2021 Boosting photocatalytic hydrogen production from water by photothermally induced biphase systems. *Nature Communications* **12**, 1343.
Gupta, K., Komal, N., Tikoo, K. B., Kumar, V., Bansal, S., Kaushik, A. & Singhal, S. 2020 Synchronous role of coupled adsorption and photocatalytic oxidation on the hybrid nanomaterials of pectin and nickel ferrite leads to the excellent removal of toxic dye effluents. *New Journal of Chemistry* **44**, 18879–18891.
Han, F. Y., Xu, X. S., Fu, Y. S. & Wang, X. 2018 Magnetically separable rice husk char-supported nickel ferrite photocatalyst with high photoactivity under visible-light irradiation. *Nano* **13**, 1850067.
Hanif, M. A., Lee, I., Akter, J., Islam, M. A., Zahid, A. A. S. M., Sapkota, K. P. & Hahn, J. R. 2019 Enhanced photocatalytic and antibacterial performance of ZnO nanoparticles prepared by an efficient thermolysis method. *Catalysts* **9**, 608.
Hariani, P. L., Said, M., Rachmat, A., Riyanti, F., Pratiwi, H. C. & Rizki, W. T. 2021 Preparation of $NiFe_2O_4$ nanoparticles by solution combustion method as photocatalyst of Congo red. *Bulletin of Chemical Reaction Engineering and Catalysis* **16**, 481–490.
Hasan, I., Bassi, A., Alharbi, K. H., Binsharfan, I. I., Khan, R. A. & Alslame, A. 2020 Sonophotocatalytic degradation of malachite green by nanocrystalline chitosan-ascorbic acid@$NiFe_2O_4$ spinel ferrite. *Coatings* **10**, 1200.
Hezam, F. A., Nur, O. & Mustafa, M. A. 2020 Synthesis, structural, optical and magnetic properties of $NiFe_2O_4$/MWCNTs/ZnO hybrid nanocomposite for solar radiation driven photocatalytic degradation and magnetic separation. *Colloids and Surfaces A: Physicochemical and Engineering Aspects* **592**, 124586.
Hossain, M., Mayanovic, R., Dey, S., Sakidja, R. & Benamara, M. 2018 Room-temperature ferromagnetism in Ni(ii)-chromia based core–shell nanoparticles: experiment and first principles calculations. *Physical Chemistry Chemical Physics* **20**, 10396–10406.
Hossein Panahi, A., Meshkinian, A., Ashrafi, S. D., Abi, G. & Kamani, H. 2020 Survey of sono-activated persulfate process for treatment of real dairy wastewater. *International Journal of Environmental Science and Technology* **17**, 93–98.
Javadmoosavi, S. Y., Naghizadeh, A., Mizwari, Z. M. & Mortazavi-Derazkola, S. 2023 Biosynthesis of novel NiFe12O19-X (X = ZnO and TiO_2) magnetic nanophotocatalyst toward the degradation pharmaceutical ceftriaxone sodium from aqueous solution under sunlight irradiation and antibacterial activity. *Ceramics International* **49**, 1351–1361.
Jiang, Z., Chen, K., Zhang, Y., Wang, Y., Wang, F., Zhang, G. & Dionysiou, D. D. 2020 Magnetically recoverable $MgFe_2O_4$/conjugated polyvinyl chloride derivative nanocomposite with higher visible-light photocatalytic activity for treating Cr(VI)-polluted water. *Separation and Purification Technology* **236**, 116272.
Kamani, H., Nasseri, S., Nabizadeh, R., Khoobi, M., Ashrafi, D., Bazrafshan, E. & Mahvi, A. H. 2018 Sonocatalytic oxidation of reactive blue 29 by N-doped TiO_2 from aqueous solution. *Journal of Mazandaran University of Medical Sciences* **28**, 157–169.
Kamani, H., Ashrafi, S. D., Jahantiq, A., Norabadi, E. & Dashti Zadeh, M. 2021 Catalytic degradation of humic acid using Fe–doped TiO_2 -ultrasound hybrid system from aqueous solution. *International Journal of Environmental Analytical Chemistry* 1–15. https://doi.org/10.1080/03067319.2021.1979535.
Kamranifar, M., Masoudi, F., Naghizadeh, A. & Asri, M. 2019 Fabrication and characterization of magnetic cobalt ferrite nanoparticles for efficient removal of humic acid from aqueous solutions. *Desalination and Water Treatment* **144**, 233–242.
Kazemi, S., Teimouri, A. & Salavati, H. 2018 Developments of modified magnetic nanoparticle-supported heteropolyacid photocatalytic performances in methylene blue scavenger. *Journal of the Chinese Chemical Society* **65**, 1218–1228.
Khan, A. U., Yuan, Q., Wei, Y., Khan, Z. U. H., Tahir, K., Khan, S. U., Ahmad, A., Khan, S., Nazir, S. & Khan, F. U. 2016 Ultra-efficient photocatalytic deprivation of methylene blue and biological activities of biogenic silver nanoparticles. *Journal of Photochemistry and Photobiology B: Biology* **159**, 49–58.
Khodadadi, M., Al-Musawi, T. J., Kamani, H., Silva, M. F. & Panahi, A. H. 2020 The practical utility of the synthesis $FeNi_3$@SiO_2@TiO_2 magnetic nanoparticles as an efficient photocatalyst for the humic acid degradation. *Chemosphere* **239**, 124723.
Kim, J. K., Alajmy, J., Borges, A. C., Joo, J. C., Ahn, H. & Campos, L. C. 2013 Degradation of humic acid by photocatalytic reaction using Nano-sized ZnO/Laponite Composite (NZLC). *Water, Air, & Soil Pollution* **224**, 1749.
Li, Y., Xu, H., Ouyang, S. & Ye, J. 2016 Metal–organic frameworks for photocatalysis. *Physical Chemistry Chemical Physics* **18**, 7563–7572.
Liu, S. Q., Feng, L. R., Xu, N., Chen, Z. G. & Wang, X. M. 2012 Magnetic nickel ferrite as a heterogeneous photo-Fenton catalyst for the degradation of rhodamine B in the presence of oxalic acid. *Chemical Engineering Journal* **203**, 432–439.
Lu, Y. B., Wang, H. C., She, X. Y., Huang, D., Yang, Y. X., Gao, X., Zhu, Z. M., Liu, X. X. & Z, X. I. E. 2021 A novel preparation of GO/$NiFe_2O_4$/TiO_2 nanorod arrays with enhanced photocatalytic activity for removing unsymmetrical dimethylhydrazine from water. *Materials Science in Semiconductor Processing* **121**, 105448.

Moein, H., Nabi Bidhendi, G., Mehrdadi, N. & Kamani, H. 2020 Efficiency of photocatalytic degradation of humic acid using magnetic nanoparticles (Fe-doped TiO_2@Fe_3O_4) in aqueous solutions. *Health Scope* **9**, e102577.

Mohammadi, N., Allahresani, A. & Naghizadeh, A. 2022 Enhanced photo-catalytic degradation of natural organic matters (NOMs) with a novel fibrous silica-copper sulfide nanocomposite (KCC1-CuS). *Journal of Molecular Structure* **1249**, 131624.

Moradi, S., Taghavi Fardood, S. & Ramazanit, A. 2018 Green synthesis and characterization of magnetic $NiFe_2O_4$@ZnO nanocomposite and its application for photocatalytic degradation of organic dyes. *Journal of Materials Science: Materials in Electronics* **29**, 14151–14160.

Mousavi, M. & Habibi-Yangjeh, A. 2016 Magnetically separable ternary g-C3N4/Fe_3O_4/BiOI nanocomposites: novel visible-light-driven photocatalysts based on graphitic carbon nitride. *Journal of Colloid and Interface Science* **465**, 83–92.

Mousavi-Kamazani, M., Zarghami, Z. & Salavati-Niasari, M. 2016 Facile and novel chemical synthesis, characterization, and formation mechanism of copper sulfide (Cu2S, Cu2S/CuS, CuS) nanostructures for increasing the efficiency of solar cells. *The Journal of Physical Chemistry C* **120**, 2096–2108.

Mustafa, F. S. & Oladipo, A. A. 2021 Photocatalytic degradation of metronidazole and bacteria disinfection activity of Ag-doped Ni0.5Zn0.5Fe2O4. *Journal of Water Process Engineering* **42**, 102132.

Nadumane, A., Shetty, K., Anantharaju, K. S., Nagaswarupa, H. P., Rangappa, D., Vidya, Y. S., Nagabhushana, H. & Prashantha, S. C. 2019 Sunlight photocatalytic performance of Mg-doped nickel ferrite synthesized by a green sol-gel route. *Journal of Science: Advanced Materials and Devices* **4**, 89–100.

Naghizadeh, A., Nasseri, S., Mahvi, A. H., Kalantary, R. R. & Rashidi, A. 2013 Continuous adsorption of natural organic matters in a column packed with carbon nanotubes. *Journal of Environmental Health Science and Engineering* **11**, 14.

Naghizadeh, A., Nasseri, S., Mahvi, A. H., Nabizadeh, R. & Kalantary, R. R. 2015 Fenton regeneration of humic acid-spent carbon nanotubes. *Desalination and Water Treatment* **54**, 2490–2495.

Naghizadeh, A., Momeni, F. & Derakhshani, E. 2017 Efficiency of ultrasonic process in regeneration of graphene nanoparticles saturated with humic acid. *Desalination and Water Treatment* **70**, 290–293.

Naik, M. M., Naik, H. S. B., Nagaraju, G., Vinuth, M., Vinu, K. & Rashmi, S. K. 2018 Effect of aluminium doping on structural, optical, photocatalytic and antibacterial activity on nickel ferrite nanoparticles by sol-gel auto-combustion method. *Journal of Materials Science-Materials in Electronics* **29**, 20395–20414.

Nawaz, M., Shahzad, A., Tahir, K., Kim, J., Moztahida, M., Jang, J., Alam, M. B., Lee, S. H., Jung, H. Y. & Lee, D. S. 2020 Photo-Fenton reaction for the degradation of sulfamethoxazole using a multi-walled carbon nanotube-$NiFe_2O_4$ composite. *Chemical Engineering Journal* **382**, 123053.

Nawaz, T., Tahir, M. B., Sagir, M., Shahzad, K., Ali, A. M. & Alrobei, H. 2022 Rapid photocatalytic degradation of dye and energy production through ternary $BiVO_4$/Ag/$NiFe_2O_4$ nanocomposites under visible light irradiation. *Ceramics International* **48**, 11779–11785.

Ojemaye, M. O., Okoh, O. O. & Okoh, A. I. 2017 Performance of $NiFe_2O_4$-SiO_2-TiO_2 magnetic photocatalyst for the effective photocatalytic reduction of Cr(VI) in aqueous solutions. *Journal of Nanomaterials* **2017**, 5264910.

Oskoei, V., Dehghani, M. H., Nazmara, S., Heibati, B., Asif, M., Tyagi, I., Agarwal, S. & Gupta, V. K. 2016 Removal of humic acid from aqueous solution using UV/ZnO nano-photocatalysis and adsorption. *Journal of Molecular Liquids* **213**, 374–380.

Pal, K., Chakroborty, S. & Nath, N. 2022 Limitations of nanomaterials insights in green chemistry sustainable route: review on novel applications. *Green Processing and Synthesis*. https://doi.org/10.1515/gps-2022-0081.

Pei, C. C. & Leung, W. W.-F. 2013 Photocatalytic degradation of Rhodamine B by TiO_2/ZnO nanofibers under visible-light irradiation. *Separation and Purification Technology* **114**, 108–116.

Perreault, F., Fonseca De Faria, A. & Elimelech, M. 2015 Environmental applications of graphene-based nanomaterials. *Chemical Society Reviews* **44**, 5861–5896.

Polshettiwar, V., Luque, R., Fihri, A., Zhu, H., Bouhrara, M. & Basset, J.-M. 2011 Magnetically recoverable nanocatalysts. *Chemical Reviews* **111**, 3036–3075.

Ren, Y.-Y., Yang, H., Wang, T. & Wang, C. 2019 Bio-synthesis of silver nanoparticles with antibacterial activity. *Materials Chemistry and Physics* **235**, 121746.

Sadeghi, M., Farhadi, S. & Zabardasti, A. 2020 Fabrication of a novel magnetic CdS nanorod/$NiFe_2O_4$/NaX zeolite nanocomposite with enhanced sonocatalytic performance in the degradation of organic dyes. *New Journal of Chemistry* **44**, 8386–8401.

Safari, G., Hoseini, M., Kamali, H., Moradirad, R. & Mahvi, A. H. 2014 Photocatalytic degradation of tetracycline antibiotic from aqueous solutions using Uv/Tio2 and Uv/H. *Journal of Health and Hygiene* **5**, 2003–2013.

Sanadi, K. R., Rathod, K. C., Gaur, M. L., Powar, R. R., Parale, V. G., Patil, R. S., Burungale, S. H. & Mali, A. V. 2021 UV light-activated photocatalytic degradation of rhodamine B dye and Suzuki cross-coupling reaction by Ni ferrite catalyst synthesized by sol–gel auto-combustion method. *Bulletin of Materials Science* **44**, 265.

Shams, S., Khan, A. U., Yuan, Q., Ahmad, W., Wei, Y., Khan, Z. U. H., Shams, S., Ahmad, A., Rahman, A. U. & Ullah, S. 2019 Facile and eco-benign synthesis of Au@Fe_2O_3 nanocomposite: efficient photocatalytic, antibacterial and antioxidant agent. *Journal of Photochemistry and Photobiology B: Biology* **199**, 111632.

Shirzadi-Ahodashti, M., Ebrahimzadeh, M. A., Amiri, O., Naghizadeh, A. & Mortazavi-Derazkola, S. 2020a Novel NiFe/Si/Au magnetic nanocatalyst: biogenic synthesis, efficient and reusable catalyst with enhanced visible light photocatalytic degradation and antibacterial activity. *Applied Organometallic Chemistry* **34**, e5467.

Shirzadi-Ahodashti, M., Ebrahimzadeh, M. A., Ghoreishi, S. M., Naghizadeh, A. & Mortazavi-Derazkola, S. 2020b Facile and eco-benign synthesis of a novel $MnFe_2O_4$@SiO_2@Au magnetic nanocomposite with antibacterial properties and enhanced photocatalytic activity under UV and visible-light irradiations. *Applied Organometallic Chemistry* **34**, e5614.

Tang, Y., Zhang, D., Li, Y., Huang, B., Li, H., Pu, X. & Geng, Y. 2019 Fabrication of magnetically recoverable Ag/$CuNb_2O_6$/$CuFe_2O_4$ ternary heterojunction composite for highly efficient photocatalytic degradation of pollutants. *Separation and Purification Technology* **220**, 78–88.

Verma, S., Arya, S., Gupta, V., Mahajan, S., Furukawa, H. & Khosla, A. 2021 Performance analysis, challenges and future perspectives of nickel based nanostructured electrodes for electrochemical supercapacitors. *Journal of Materials Research and Technology* **11**, 564–599.

Vijay, S., Balakrishnan, R. M., Rene, E. R. & Priyanka, U. 2019 Photocatalytic degradation of Irgalite violet dye using nickel ferrite nanoparticles. *Journal of Water Supply Research and Technology-Aqua* **68**, 666–674.

Wang, J., Ding, S., Zheng, C., Ma, H. & Ji, Y. 2012 Efficient removal of humic acid in aqueous solution using polyaniline adsorbent. *Desalination and Water Treatment* **40**, 92–99.

Wang, Q., Huang, S., Cui, X., Zhang, Q., Zhang, J. & Chen, Z. 2022 Constructing recyclable $NiFe_2O_4$/MoS_2 Z-scheme photocatalysts with enhanced catalytic activity. *Journal of Materials Science* **57**, 3525–3537.

Wu, Q. 2020 Fabrication of black $TiO_2 - x/NiFe_2O_4$ supported on diatomaceous earth with enhanced sonocatalytic activity for ibuprofen mitigation. *Nanotechnology* **32**, 055706.

Xiao, L., Liu, J. & Ge, J. 2021 Dynamic game in agriculture and industry cross-sectoral water pollution governance in developing countries. *Agricultural Water Management* **243**, 106417.

Xie, Z., Peng, Y.-P., Yu, L., Xing, C., Qiu, M., Hu, J. & Zhang, H. 2020 Solar-inspired water purification based on emerging 2D materials: status and challenges. *Solar RRL* **4**, 1900400.

Yan, K., Wu, X., An, X. & Xie, X. 2013 Facile synthesis and catalytic property of spinel ferrites by a template method. *Journal of Alloys and Compounds* **552**, 405–408.

Yeganeh, F. E., Yousefi, M., Hekmati, M. & Bikhof, M. 2020 Photocatalytic degradation of coomassie blue G-250 by magnetic $NiFe_2O_4$/ZnO nanocomposite. *Comptes Rendus Chimie* **23**, 385–393.

Zhou, T. H., Zhang, G. Z., Zhang, H. W., Yang, H., Ma, P. J., Li, X. T., Qiu, X. L. & Liu, G. 2018 Highly efficient visible-light-driven photocatalytic degradation of rhodamine B by a novel Z-scheme Ag_3PO_4/MIL-101/$NiFe_2O_4$ composite. *Catalysis Science & Technology* **8**, 2402–2416.

First received 19 May 2023; accepted in revised form 15 July 2023. Available online 7 August 2023